

# Estimation and Study of Biological Tissues Using Optical Methods

G. Jagajothi

Mount Zion College of Engineering and Technology, Pudukkottai, India

**Abstract:** The laser radiation is increasingly applied in therapeutic and diagnostic medicine to detect the abnormal tissue non-invasively and for the treatment of different pathologies in tissues. When this radiation is incident on a tissue, due to mismatch in refractive index at the air-tissue interface, a part of this beam is specularly reflected, whereas, the remaining part enters the tissue. Experimental result using circular saline photons showed the feasibility of the method for biomedical applications such as the study of characterization of biological tissues and wound healing. Because of cellular tissue structure and refractive index variation in the tissues beneath, some photons emerge from the surface (backscattering) and the rests are absorbed in thick complex tissues. In soft tissues such as human breast a part of this beam is also transmitted. The penetration of light within the 'therapeutic window' is more leading to high remittance after deep penetration which could be probed to measure the metabolic, physiologic or possibly structural status of tissues. On the other hand the transmitted component also carries the information on the structural variation but this is partially blurred due to high scattering nature of tissues.

**Keywords:** Tissue Medium, Optical Properties, 820 nm laser diode, MC simulation, ANN and diffuse scattering light

## 1. Introduction

Successful application of lasers in medicine warrants a thorough understanding and knowledge about the complex photon tissue interactions. When laser light is incident on a tissue, a fraction of this emerges as backscattered component at various locations on the tissue surface. For most of the biological tissues, the scattering process dominates within therapeutic window region (600-1300 nm). There is a need for solid tissue – equivalent phantoms which could simulate the inhomogeneous characteristics of biological tissues and at the same time allow easy tuning of optical properties are discussed [1]. Optics for laser irradiation of tissue is best described by examining the response of a target within the tissue. Suppose the tissue (e.g. skin) has a chromosphere somewhere inside the tissue at coordinate  $r$  with respect to some frame of reference as shown in Fig.1.1. The characteristics of photon propagation, which include scattering and absorption events within tissue and reflection and transmission at boundaries, govern the number of photons that would be the melanocyte at coordinate  $r$ . For example, consider the paths of two photons that would reach the target chromophore as illustrated in Fig. 1.2. The changes in direction of propagation shown in the figure suggest that quite a large number of scattering events take place for each photon. At visible and near – IR wavelength (600-1300 nm) [2] light scattering is an important phenomenon in tissue, and the average distance a photon travels between two scattering events is about 0.05 to 0.2 mm. When a laser beam sequentially scans tissue, moving blood cells generate the signals components in the backscattered light. A photodiode detects a fraction of this back-scattered light, and the signals proportional to the perfusion in each measurement point is calculated and stored in a computer memory. Detection of breast lesions in trans-illumination images by the use of red or NIR light is of particular medical interest [3].

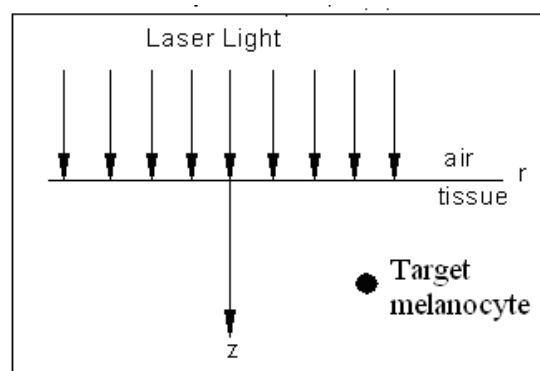


Figure 1.1: Light propagation in Tissue Medium

## 1.2 Optical Properties

The position of a single light spot is determined from the current signals obtained from the four active terminals of the photodiode. The position of each light spot is determined sequentially, and each value is stored by an Integrated Circuit(IC) sample and hold amplifier. Analog differencing used to obtain one signal proportional is found to be the  $x_1-x_2$  light spot separation, and another proportional to the  $Y_1-Y_2$  light spot separation.

Photodiode is a circular and large area photodiode has four active electrical terminals and one bias connection. The active terminals are arranged in two pairs, each along a perpendicular (X and Y) axis. When a single light spot is directed onto the photosensitive surface, currents are generated in the active terminals, with the current in a given terminals being proportional to both the intensity of the light spot and the proximity of the light spot to the terminal. Since the photodiode has a greater responsivity to light in the IR range, an IR emitter with a peak wavelength of 820 nm is used as the light source. In addition an IR optical filter is placed above the light sensitive surface of the photodiode. Near-infrared (NIR) light is strongly scattered inside most biological tissues, so the diffusion equation has been widely

Volume 8 Issue 3, March 2019

[www.ijsr.net](http://www.ijsr.net)

Licensed Under Creative Commons Attribution CC BY

employed in studies focused on NIR imaging and spectroscopy [4].

Photons in a turbid medium move in all directions and may be scattered or absorbed. The absorption and scattering coefficients are defined such that when a photon propagates over infinitesimal distance  $ds$ , the probability for absorption or scattering is respectively as follows, The probability of absorption in infinitesimal distance  $ds$  is  $\mu_a ds$ , The probability of scattering in infinitesimal distance  $ds$  is  $\mu_s ds$ , The mean free path for an absorption event is  $1/\mu_a$  and the mean free path for a scattering event is  $1/\mu_s$ . The sum of  $\mu_a$  and  $\mu_s$  is designated as the total attenuation coefficient,  $\mu_t$

$$\mu_t = \mu_a + \mu_s \quad (1)$$

Thus the probability that a photon is absorbed in a distance is less than  $S_i$  denoted by the Probability  $P(s < s_i)$ , is

$$P(s < s_i) = 1 - e^{-\mu_a s} \quad (2)$$

where this probability defines a probability distribution function is denoted by  $F(s_i)$ .

## 1.2 Reflection and Transmission at a Surface

The interaction of laser light with tissue is highly dependent upon the method for delivery of the laser energy to a selected target.

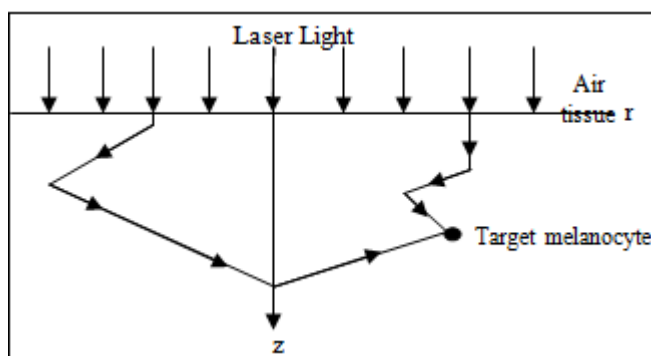


Figure 1.2: Light path in a tissue with anomaly directions

A portion of light beam is reflected at the surface due to the difference in the index of refraction,  $n_1=1$ , of the air and the index of the refraction,  $n_2=1.4$ , of the tissue, according to the laws of Fresnel. The fraction of light that is directly reflected from the surface depends upon the angle of incidence of the laser beam and the two indices of refraction. Even when the laser beam is perpendicular to the tissue, a small fraction is reflected. Non-invasive [5] characterization of tissues by a light sources of great importance for the diagnostic and therapeutic applications. Diffuse Reflectance Spectroscopy provides a straightforward and simple approach for optical tissue differentiation [6]. Proper use of lasers in medicine needs a thorough understanding and knowledge about the mechanism on complex photon tissue interaction mechanisms. When laser light is incident on a tissue, a fraction of light emerges as backscattered component at various locations on the tissue surface. The spatial distribution of the backscattered component provides information on variation in internal composition of the tissue. Monte Carlo simulation and experiments in tissue phantoms were used to empirically develop an analytical model that

characterizes the reflectance spectrum in a turbid medium [7]. For thin complex tissues such as hand and thick-soft tissues like as the human breast, a part of the incident beam is diffusely transmitted, which also contains information on their internal structures. A new diagnostic or therapeutic technique needs a thorough evaluation in terms of their potential, limitations, and patient safety prior to putting them into clinical practice. In this context, tissue-equivalent optical phantoms could play an important role in evaluating a new optical diagnostic technique. Research on both diagnostic and therapeutic microwave techniques benefits from anatomically realistic numerical breast phantoms that model structural complexities, tissue heterogeneity, and dispersive dielectric properties [8]. Since most of the imaging techniques are time consuming, biological tissues lose their optical characteristics with time once they are harvested away from the human body. Therefore, it becomes necessary to develop tissue equivalent optical phantoms which do not lose their characteristics with time for evaluation of these new techniques. Measurements were taken at selected source-detector offsets, using slab like diffusely scattering and fluorescent phantoms containing fluorescent heterogeneities [9]. For most of the biological tissues, the scattering process dominates within the therapeutic window region (600-1300nm). Most of these phantoms are liquids, which do not allow uniform distribution of scattering of particles within the medium and are not stable over long periods of time. These liquid phantoms do not allow inclusion of optical inhomogeneities mimicking clinical lesions. To overcome the difficulties associated with liquid phantoms, solid tissue-equivalent phantoms came to the forefront.

## 1.3 Back Scatter

When a laser beam is incident on tissue, a small amount of light would be reflected from the surface. This is due to the slight divergence of the laser beam and roughness of the tissue surface. Inside the tissue, scattering and absorption attenuate the collimated beam and further de-collimate the incident flux as photons are scattered away from the laser beam. Some of the light scattered from the collimated beam undergoes multiple reflections and propagates in the backward directions. Backscattered light that reaches the tissue surface is either internally reflected or transmitted according to Fresnel's relation. Optical measurements have been extended with light that is modulated at near-gigahertz frequencies, with the expected advantages of better contrast and resolution in the images [39]. Thus, any measurement of reflection includes both the specular reflection above the irradiated tissue and the transmitted portion of the backscattered flux. That is,

$$R_t = r + R_d \quad (3)$$

where  $R_t$  is the total reflectance,  $r$  is the specular reflection and  $R_d$  is the diffuse reflectance.

## 1.4 Reflection of Diffuse Light

Diffuse light corresponds to a constant radiance for any directions. That is,

$$L(r, s) = L(r) \quad (4)$$

If a surface is irradiated uniformly with diffuse light, the total integrated incident power per unit area, or the flux, was calculated using

$$E_d = F_{n+} = \lambda L [W/m^2] \quad (5)$$

For n into the medium.

The reflected power for rays of incident light between  $\theta_1$  and  $\theta_1 + d\theta_1$  is

$$r(\theta_1)L \cos \theta_1 2\pi \sin \theta_1 d\theta_1 \quad (6)$$

where  $r(\theta_1)$  is the Fresnel reflection coefficient at angle  $\theta_1$ . The total reflected power is obtained by integrating Eqn.(6) over  $\theta$  from 0 to  $\pi/2$ :

$$2\lambda L \int_0^{\lambda/2} r(\theta_1) \cos \theta_1 \sin \theta_1 d\theta_1 = \lambda L \int_0^{\lambda/2} r(\theta_1) \sin(2\theta_1) d\theta_1 \quad (7)$$

The integrated specular reflection coefficient  $r_{sd}$  for diffuse irradiance of tissue from air is

$$r_{sd} = \frac{\text{reflected power}}{\text{incident power}} \quad (8)$$

for uniform diffuse irradiance, Eqs(7) and (8) yield

$$r_{sd} = \int_0^{\lambda/2} r(\theta_1) \sin(2\theta_1) d\theta_1 \quad (9)$$

The above equation can be modified to compute internal reflection of light at tissue – air interfaces by including the critical angle for total internal reflection,  $\theta_c$ . For light traveling to the surface at an angle ( $\theta_i > \theta_c$ ), the Fresnel reflection coefficient is equal to 1.

## 2. Propagation of Light into Tissue

### 2.1 Collimated Light

Light entering the tissue is subject to scattering and absorption. The attenuation losses of standard visible and near-IR fibres (in the usual case they are much less than 1 dB/km), the typical attenuation losses of IR fibres are a few orders of magnitude larger (approximately  $10^2 - 10^4$  dB/km) [40]. A collimated laser beam normal to the surface has a small portion of the light reflected at the surface and the remaining light is attenuated in the tissue by absorption and scattering according to Beer's Law;

$$E(z) = E_0 (1 - r_{sc}) e^{-(\mu_a + \mu_s)z} \quad (10)$$

where  $E(z)$  is the fluence rate of collimated light at position  $z$  in the tissue  $W/m^2$  sometimes denoted as the primary fluence rate,

$$\phi(z) = E(z) \quad (11)$$

$E_0$  is collimated irradiance  $W/m^2$ ,  $r_{sc}$  is the Fresnel surface reflection of collimated light striking the external surface.

### 2.2 Rules for Photon Propagation

The photon propagation in biological tissue using Monte Carlo model was used. A Monte Carlo Simulation that uses a weighted photon to improve the statistics of the simulation. The Monte Carlo method has been applied to numerical modeling of an integration sphere designed for

hemispherical-directional reflectance factor measurement [10]. The rules of the light propagation in the tissue medium are given below. The photon is initialized with a weight of unity. The distance of the photon's step to the first interaction event is found and the photon is moved. If the photon has left the tissue, the possibility of internal reflectance is checked. If the photon is internally reflected, then the photon position is adjusted accordingly and the programme continues, otherwise the photon escapes and the event is recorded as observable reflectance (or transmittance). With each step, the photon's weight is decremented. The fraction of lost weight is added to the local element of an array associated with the position of the photon that indicates photon energy absorbed by the tissue. A super-luminescent diode (SLD) is used as the light source whose spectral width  $\Delta\lambda$  is 16 nm (FWHM) at the center wavelength  $\lambda_c = 850$  nm [11]. The remaining photon weight is then scattered statistically to achieve a new direction, and a new step is calculated. If the photon weight falls below a threshold minimum value, then roulette is played to either extinguish the photon or continue propagating the photon.

### 2.3 Propagation of Scattered Light

If tissues were just light absorbing media, that would be non-scattering, the resulting light distribution following laser irradiation could easily be described by a simple Beer's law. Only an absorption coefficient would be required to compute the distribution of light in tissue. A Monte Carlo simulation package was developed to study the generation and subsequent propagation of fluorescent light within human skin tissue [12]. However, that tissues are somewhat whitish material rather than black, demonstrating that they scatter visible light. Scattering is usually caused by random spatial variations in tissue density, refractive index and dielectric constant and actual light distributions can be substantially different from distributions estimated using Beer's law. Also, scattering extends the light fluence rate beyond the lateral dimensions of the incident irradiance. The magnitude of these effects and their importance depends rather than strongly on (i) The scattering and absorbing properties of the tissue and (ii). The diameter of the laser spot is related to the penetration depth of the light. Most important, the scattering coefficient and absorption coefficient are wavelength dependent. The absorption coefficient of tissue can vary strongly over the wavelength range of clinical laser medicine while the scattering coefficient decreases monotonically with wavelength. The ratio of these coefficients can also vary substantially with (laser) wavelength. Light scattered from the collimated beam undergoes multiple scattering events as it propagates through the tissue. A rigorous description of this propagation in terms of Maxwell's wave equations is not possible at this time. An approach that has proven effective is the transport equation that describes the transfer of energy through a turbid medium.

### 2.4 MC Modeling of Light Transport in Tissues

Monte Carlo Simulations of photon propagation offer a flexible yet rigorous approach toward photon transport in

turbid tissues. This method simulates the random walk of photons in a medium that contains absorption and scattering. Monte Carlo simulations for multi-layered media (MCML) is included (i) fluorescence photon generation and propagation in tissues, and (ii) excitation that photon propagation in the half-ball lens and fluorescence photon collection by the half-ball lens and the beveled-tip collection million fiber [13]. The method is based on a set of rules that govern the movement of a photon in the tissue. The two key decisions are: (i) the mean free path for a scattering or absorption event, and (ii) the scattering angle. The rules of photon propagation are expressed as probability distributions for the incremental steps of photon movement between sites of photon tissue interactions, for the angles of deflections in a photon trajectory when a scattering event occurs and for the probability of transmittance or reflectance at boundaries. Monte Carlo light propagation is rigorous yet very descriptive. Monte Carlo calculations can solve problems of real life that are otherwise difficult or even impossible. Its ability to simulate any 3D geometry enables its use for clinical routine radiotherapy treatment planning [14-16]. This method is basically statistical in nature and requires a computer to calculate the propagation of a large number of photons.

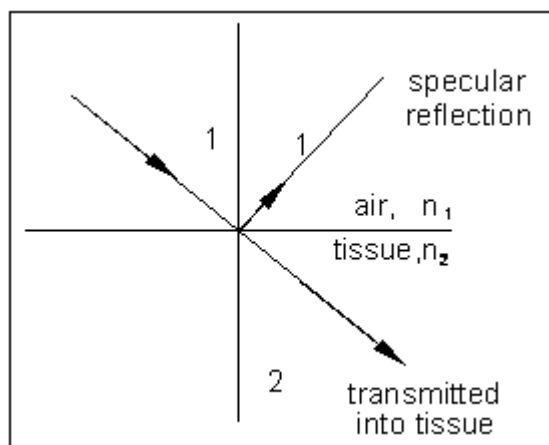


Figure 1.3: Light propagation in the air and tissue medium

The number of photons required in a simulation depends largely on the question being asked, the precision needed, and the spatial or temporal resolution desired. For example, to simply learn the total reflectance,  $R_t$  from a tissue of specified optical properties, typically about 3,000 photons can yield a useful result. To map the spatial distribution of photons,  $\phi(r,z)$ , in a radially symmetric problem at least 10,000 photons are usually required to yield an acceptable answer. To map spatial distributions in a more complex three dimensional problem such as a finite diameter beam irradiating a tissue with a buried blood vessel [17], the required photons may exceed 100,000. The main point in these introductory remarks is that Monte Carlo simulations are rigorous, yet statistical and therefore require significant computation time to achieve a specified precision and resolution.

The details of the grid element organization for accumulating data would be delayed for layer. The arrays would simply be

referenced by the location of the grid element,  $(x, y, z)$  rather than by the indices of the grid element,  $[i,j,k]$ .

## 2.5 Launching the Photon

Each photon is initially assigned a weight,  $W$ , equal to unity. The photon is injected orthogonally into the tissue at the origin, which corresponds to a collimated ray of incident photons. When the photon is launched, if there is a mismatched boundary at the tissue surface, then some specular reflectance would occur. A fundamental understanding of the origin of light scattering from biological cells is relevant to a number of noninvasive medical diagnostic techniques for cancer and for other tissue pathologies. If the refractive indices of the outside medium and tissue are  $n_1$  and  $n_2$  respectively, then the specular reflectance,  $R_{sp}$  is specified as;

$$R_{sp} = \frac{(n_1 - n_2)^2}{(n_1 + n_2)^2} \quad (12)$$

The photon weight is decremented by  $R_{sp}$

$$W = 1 - R_{sp} \quad (13)$$

The specular reflectance is stored as the parameter  $R_{sp}$ , and is used when considering total reflectance in contrast to diffuse reflectance. Subsequent discussion of reflectance refers to the diffuse reflectance due to photons that entered the tissue and later escaped. They found the optical properties of normal and malignant human breast tissues. They used diffused reflectance measurements method to trace out. In this method, they used PMT instead of amplifier. Also, they used He-Ne Laser to find the tissue properties. In this work, 820 nm laser source has been used to collect the back scattered light.

## 2.6 Photon Step Size, S

The step size of the photon,  $s$ , is calculated based on a random sampling of the probability density function for  $s$ . The computer's random number generator yields a random variable.

## 2.7 Moving the Photon

Once  $s$  is specified, the photon is ready to be moved in the tissue, and it is ready to be moved in the tissue. The present position of the photon is specified by  $(x, y, z)$ . The current trajectory of the photon is specified by a unit vector,  $r$ , which is characterized by the direct cosines  $(\mu_x, \mu_y, \mu_z)$ , the following equations represent,

$$\mu_x = r \cdot x \quad (13)$$

$$\mu_y = r \cdot y \quad (14)$$

$$\mu_z = r \cdot z \quad (15)$$

where  $x, y$  and  $z$  are unit vectors along each axis. At launching, the photon position is  $(0, 0, 0)$  and the trajectory is  $(0, 0, 1)$ . The new position of the photon is specified by  $(x', y', z')$  and is calculated:

$$x' = x + \mu_x s \quad (16)$$

$$y' = y + \mu_y s \quad (17)$$

$$z' = z + \mu_z s \quad (18)$$

## 2.8 Photon Absorption

Volume 8 Issue 3, March 2019

[www.ijsr.net](http://www.ijsr.net)

Licensed Under Creative Commons Attribution CC BY

Once the photon has taken a step, some attenuation of the photon weight due to absorption by the tissue must occur. The amount of deposited photon weight is  $\Delta Q = W \mu_a / \mu_t$ . The current value  $Q(x,y,z)$ , for the total accumulated photon weight is previously deposited in the local grid element  $(x,y,z)$  is updated.

$$Q(x,y,z) \leftarrow Q(x,y,z) + \Delta Q \tag{14}$$

The new photon weight,  $W$  is calculated

$$W \leftarrow W \mu_s / \mu_t \tag{15}$$

Note that  $(\mu_a / \mu_t + \mu_s / \mu_t)$  equals to unity. Hence the energy is conserved.

### 2.9 The Basic Idea

The basic strategy of this implementation of the Monte Carlo method is to record the accumulated photon energy density,  $Q$ , in L/cc that is deposited in a local tissue volume. The local light fluence,  $\phi$ , in J/cm<sup>2</sup> is calculated using the local absorption coefficient,  $\mu_a$ , in cm<sup>-1</sup>

$$\phi = Q / \mu_a \tag{16}$$

### 2.10 The Grid Elements

A cylindrical coordinate system requires two variables ( $r, z$ ) while a Cartesian coordinate system requires three variable ( $x, y, z$ ). Also, equally spaced grids have been chosen because the resulting plots of iso-fluence. Contours are smooth at positions distant from the source at the origin. In contrast, logarithmically scaled grid sizes offer better resolution near the source but the poor resolution at distant point. Let us organize the grid in cylindrical coordinates as array,  $Q[i,j]$ , which corresponds to the accumulated energy deposition,  $Q[r,z]$  in units of photon weight. Photon propagation is conducted in Cartesian coordinates of  $x, y$  and  $z$ . The coordinate  $r$  is given by,

$$r = \sqrt{x^2 + y^2} \tag{17}$$

which always yields a positive value for  $r$ . All values of  $z$  are positive within the tissue slab. The grid element  $[i, j]$  corresponds to the position  $(r,z)$  such that,

$$idr \leq r < (i+1) dr \tag{18}$$

$$jdz \leq z < (j+1) dz \tag{19}$$

If the computer language offers an INTEGER function that rounds off 2.49 to 2 and 2.50 to 3, then the following assignment statements are used:

$$i = \text{INTEGER}(r/dr - 0.5) \tag{20}$$

$$j = \text{INTEGER}(z/dz - 0.5) \tag{21}$$

and INTEGER of a negative number equals to zero.

The following figure shows the penetration of light at various levels.

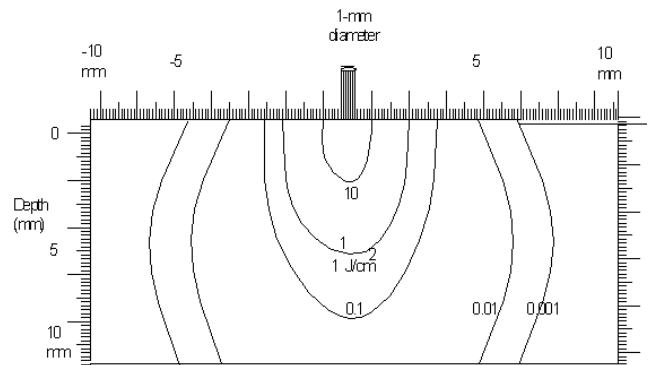


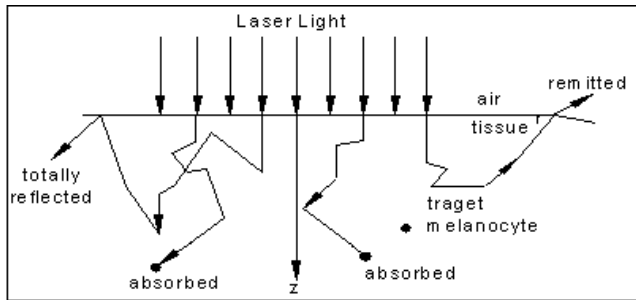
Figure 1.4: Penetration of light with different depths

### 2.11 Light Propagation in Tissue

Modeling light scattering is essential for establishing dosimetry for photochemical reactions in tissue such as in Photodynamic Therapy (PDT). Typically excitation wavelengths for PDT are between 600 and 800 nm to maximize penetration of laser light into the tissue. In this limited spectrum, absorption is typically much less than scattering. The key dosimetry parameter for PDT is the fluence rate  $\phi(r)$ . Typically, the laser spot size for PDT in the skin is large, to cover as much of the lesions as possible and reduce the number of individual spots that must be treated, in these cases the spot size is much larger than the effective penetration depth. The collected light carries the absorption structure of trace gases that are present along the light path; these structures can be detected with high sensitivity.

### 2.12 Diagnosis

An important use of lasers is their application to diagnostic problems. This class of problems includes the use of light to either identify the status of the tissue or to classify tissue. Because of the wavelength dependence of the optical properties of the tissue, the measured fluorescence line shape is not equal to the intrinsic line shape of the fluorochromophore. By using Monte Carlo model it is possible to simulate the effects of the tissue attenuation tissue sample geometry, and detector field of view and alignment. Transport theory, and Monte Carlo techniques to support the remarkable progress in developing optical tomographic techniques in recent years. The optical modeling results described here and are obtained two Monte Carlo simulations a single photon variable step size model for the excitation ray and a weighted photon, variable step size model for the fluorescence and Table 1. Shows Monte carlo simulation with the standard data. The photons absorbed at various depths of the tissue have been computed. The points that were already at the grid points, without any interpolation of these have been carried out. To understand the accuracy of the estimates for  $\mu_s$  and  $\mu_a$  from the diffuse reflectance data, we first made measurement of tissue phantoms with known optical transport parameters.



1.5 Sub-sub Section Head Style

These procedures have been repeated for the wavelength region at 820nm. The present study shows the backscattering from the biological tissues that depend on their composition and blood flow. The incidence light on the phantom is in the form of thin sheath of light but the transmitted component is received after a fixed separation. Because of this, the contribution due to scattering at the detector is increased. The reconstructed images of spatial variation of the backscattered intensity or depth variation of photons provided valuable data on the type, size and locations of abnormal tissue. In this paper we consider locations and sizes of anomalies as the core information to search for and focus our attention on the fast and accurate estimation of them. MC Simulation is a statistical technique for simulating random processes and has been applied to light tissue interactions under wide variety of simulations.

### 3. Results

The obtained results were compared and analysed with the following five algorithms as shown in Table 1.

S.No	Types of Algorithm	Performance Rate
1	Variable Learning Rate (traingda, traingdx)	$1.98858 \times 10^{-5}$
2	Resilient Back propagation (trainrp)	$9.0158 \times 10^{-6}$
3	Conjugate Gradient Algorithms	$4.05839 \times 10^{-6}$
4	Quasi-Newton Algorithms	$6.66356 \times 10^{-7}$
5	Levenberg-Marquardt (trainlm)	$4.69968 \times 10^{-9}$

**Table 2:** Shows the comparison of simulation and experimental Value and phantom value as obtained from various methods

S.No	Tissues	Simulation value	Experimental value	Phantom value
1	Muscle	0.0305826	0.032	0.034
2	Skin	0.0716	0.072	0.074
3	Bone	0.03835	0.038	0.039
4	Fat	0.072956	0.065	0.068
5	Tendon	0.0315626	0.030	0.032
6.	Vessie	0.0632	0.064	0.064
7.	Nerve	0.0732	0.0754	0.078

### 4. Conclusion

The light propagation in biological tissues in turbid medium was analyzed using Monte Carlo Simulation method. While the earlier researchers have obtained diffuse reflectance ( $r_d$ ) through Monte Carlo Simulation, here diffuse reflectance ( $r_d$ ), back scattered reflectance, depth and heat absorption also have been obtained additionally.  $10^6$  photons are used as

reference to study the various coordinates. Using simulation programme, obtained various graphs for absorption, transmission and reflectance have been obtained. These graphs prove that values of normal tissue are slightly varied from that of abnormal tissues. The harvested human biological tissues as obtained earlier are soaked both in saline and formaldehyde solutions to preserve and to get the normal value. Then, these tissues are measured using laser reflectometry method. The data obtained from laser reflectometry is then compared with ANN simulation software. Monte Carlo Simulated results of optical parameters in biological tissues are compared and found that these values are matching with the existing values.

### References

- [1] Wai-Fung Cheong, Scott A. Prahl, and Ashley and J. Welch, Senior member, IEEE, "A Review of the Optical Properties of Biological Tissues," *IEEE Journal of Quantum Electronics*, Vol.26.No.12, pp.2166-2185,1990.
- [2] R.Srinivasan and Megha Singh, "Laser Backscattering and Transillumination Imaging of Human Tissues and Their Equivalent Phantoms," *IEEE Trans. Biomed. Eng.*, Vol.50,no.6, pp.724-730,2003.
- [3] D. Grosenick, H. Wabnitz, and H. Rinneberg, "Time-Resolved imaging of solid phantoms for optical mammography," *Applied Optics*, Vol.36,No.1, pp.221-231,1997.
- [4] Sergio Fantini, Maria Angela Franceschini, and Enrico Gratton, "Effective source term in the diffusion equation for photon transport in turbid media," *Applied Optics*, Vol.36,No.1,pp. 156-163,1997.
- [5] D. Kumar and M. Singh, "Non-invasive imaging of optical parameters of biological tissues," *Med. Biol. Eng. Comput.*, Vol.41,pp.310-316,1996.
- [6] Azhar Zam, Florian and Stelzle, et al., "Soft tissue differentiation by diffuse reflectance spectroscopy," *SPIE-OSA*, 738, pp.736821-1 – 5,2009.
- [7] Roberto Reif, Ousama A'Amar, and Irving J. Bigio, "Analytical model of light reflectance for extraction of the optical properties in small volumes of turbid media," *Applied Optics*, Vol.46,No.29, pp.7317-7328,2007.
- [8] Earl Zastrow, Student Member, IEEE, Shakti K. Davis, Member, IEEE, Mariya Lazebnik, Student Member, IEEE, Frederick Kelcz, Barry D. Van Veen, Fellow, IEEE, and Susan C. Hagness, Senior Member, IEEE, "Development of Anatomically Realistic Numerical Breast Phantoms With Accurate Dielectric Properties for Modeling Microwave Interactions With the Human Breast," *IEEE Transactions on Biomedical Engineering*, Vol.55,No.12, pp.2792-2880,2008.
- [9] Ronny Ziegler, Tim Nielsen, Thomas Koehler, Dirk Grosenick,Oliver Steinkellner, Axel Hagen, Rainer Macdonald, and Herbert Rinneberg, "Nonlinear reconstruction of absorption and fluorescence contrast from measured diffuse transmittance and reflectance of a compressed-breast-simulating phantom," *Applied Optics*, Vol.48,No.24, pp.4651-4662,2008
- [10] S. B. Colak, D. G. Papaioannou, G. W. 't Hooft, M. B. van der Mark, H. Schomberg, J. C. J. Paasschens, J. B.

- M. Melissen, and N. A. J. van Asten, "Tomographic image reconstruction from optical projections in light-diffusing media,
- [11] Ilko K. Ilev, Ronald W. Waynant, and Michael A. Bonaguidi, " Attenuation measurement of infrared optical fibers by use of a hollow-taper-based coupling method, " *Applied Optics*, Vol.39 ,No.19 , pp.3192-3196,2000.
- [12] Alexander V. Prokhorov, Sergey N. Mekhontsev, and Leonard M. Hanssen, " Monte Carlo modeling of an integrating sphere Reflectometer," *Applied Optics*, Vol.42,No.19, pp.3832-3842,2003.
- [13] Masato Ohmi, Yasuhito Ohnishi, Koji Yoden, and Masamitsu Haruna, " *In Vitro* Simultaneous Measurement of Refractive Index and Thickness of Biological Tissue by the Low Coherence Interferometry," *IEEE Transactions on Biomedical Engineering*, Vol.47,No.9, pp.1266-1270,2000.
- [14] Michael J. McShane, Member, IEEE, Sohi Rastegar, Michael Pishko, and Gerard L. Coté, Senior Member, IEEE, "Monte Carlo Modeling for Implantable Fluorescent Analyte Sensors, " *IEEE Transactions On Biomedical Engineering*, Vol.47,No.5,pp. 624-632,2000.
- [15] Franck Jaillon, Wei Zheng, and Zhiwei Huang, "Half-ball lens couples a beveled fiber probe for depth-resolved spectroscopy: Monte Carlo simulations, " *Applied Optics*, Vol.47,No.17, pp.3152-3157, 2008.
- [16] Sonia M. Reda1, Eman Massoud, Magda S. Hanafy1, Ibrahim I. Bashter1 and Esmat A. Amin, " Monte Carlo Dose Calculations For Breast Radiotherapy Using 60co Gamma Rays," *Journal of Nuclear and Radiation Physics*, Vol.1,No.1, pp.61-72,2006.
- [17] Judith R. Mourant, James p. Freyer, Andreas H. and Hielscher, et at., "Mechanisms of light scattering from biological cells relevant to noninvasive optical-tissue diagnostics," *Applied optics*, Vol.37,No.16, pp.3586-3593,1998.